Advancing Toxicokinetic-Toxicodynamic Modeling to Assess Kinetic Bioavailability in Sediments

Journal:	*Environmental Science & Technology*
Manuscript ID	es-2025-114943
Manuscript Type:	Article
Date Submitted by the Author:	19-Aug-2025
Complete List of Authors:	Lin, Zhi; Xiamen University, College of the Environment and Ecology Xiao, Wenze; Xiamen University, College of the Environment and Ecology Tan, Qiao-Guo; Xiamen University, College of the Environment and Ecology Simpson, Stuart; CSIRO Environment Business Unit, Industry Environments Chen, Rong; Xiamen University, College of the Environment and Ecology Wang, Wen-Xiong; City University of Hong Kong, School of Energy and Environment Xie, Minwei; Xiamen University, College of the Environment and Ecology

Advancing Toxicokinetic-Toxicodynamic Modeling to Assess Kinetic Bioavailability in Sediments

Zhi Lin[1], Wenze Xiao[1], Qiao-Guo Tan[1], Stuart L. Simpson[2], Rong Chen[1], Wen-Xiong Wang[3], Minwei Xie[1*]

1. Fujian Provincial Key Laboratory for Coastal Ecology and Environmental Studies, State Key Laboratory of Marine Environmental Science, Key Laboratory of the Ministry of Education for Coastal and Wetland Ecosystem, College of the Environment and Ecology, Xiamen University, Xiamen, Fujian, 361102, China
2. CSIRO Environment, Ecosciences Precinct, 41 Boggo Road, QLD 4102, Australia
3. School of Energy and Environment, State Key Laboratory of Marine Pollution, City University of Hong Kong, Hong Kong 999077, China

*Corresponding Author: minweixie@xmu.edu.cn

TOC Art

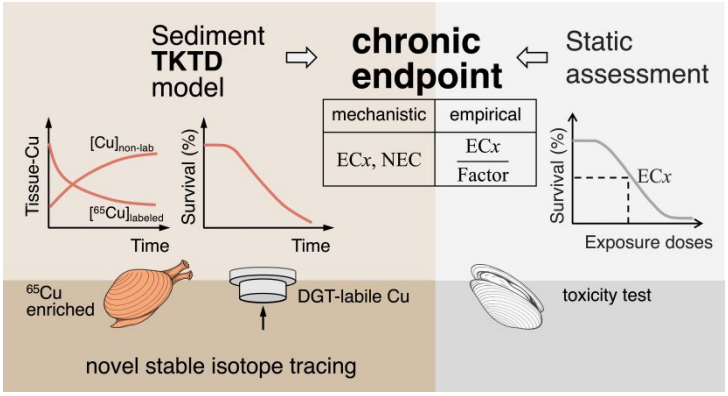
Sediment
TKTD
model
chronic
endpoint
Static
assessment
mechanistic
empirical
ECx, NEC
ECx
Factor
Tissue-Cu
[Cu]non-lab
[65Cu]labeled
Time
Survival (%)
Time
Survival (%)
ECx
Exposure doses
65Cu
enriched
DGT-labile Cu
toxicity test
novel stable isotope tracing

Abstract

Traditional sediment risk assessments often rely on fixed-duration dose-response endpoints, which overlook how exposure conditions and organismal response interact over time. Toxicokinetic-toxicodynamic (TKTD) models address this by linking external exposure, internal concentration, and effects, but their application to sediments has been limited by the lack of suitable tracing methods to generate high-quality kinetic data. Here, we developed a novel stable isotope tracing approach tailored for sediment TKTD studies—pre-labeling clams with stable ^{65}Cu in water prior to Cu-amended sediment exposure. By simultaneously tracking ^{65}Cu elimination and ambient Cu uptake, we successfully established a sediment TKTD model that reproduced bioaccumulation and toxicity across a wide range of Cu bioavailability driven by speciation differences. The model revealed that *Ruditapes philippinarum*'s Cu elimination and tolerance capability were consistent across exposure conditions, indicating species-specific physiological traits. Cu uptake followed a saturation-type Michaelis-Menten relationship with bioavailable Cu. From these kinetics, we derived mechanistic bioavailability benchmarks—DGT-Cu based LC_{50}-chronic = 46 μg L^{-1} and NEC_{DGT} = 40 μg L^{-1}—as chronic thresholds applicable to risk assessment. Overall, this study demonstrates TKTD modeling in sediments using stable isotope tracing, advancing process-based ecological risk assessments and providing a transferable framework for evaluating contaminant bioavailability in estuarine ecosystems.

Keywords: Process-based model, sediment risk assessment, Cu speciation, *Ruditapes philippinarum*

Synopsis:

By designing a novel stable isotope tracing technique, we established a sediment TKTD model, advancing bioavailability-based risk assessment for contaminants in dynamic estuarine environments.

1. Introduction

In estuarine and coastal ecosystems, sediments can store anthropogenic contaminants that later remobilize,[1–3] causing prolonged harm to benthic and pelagic communities.[4,5] Chronic risk assessment is therefore essential for informing sediment remediation, habitat restoration, and long-term pollution control.[6] Most conventional sediment risk assessments, however, use static dose-response models to derive the fixed-duration endpoints (e.g, 10-d ECx, where ECx represents x% effect concentration).[7–9] When chronic toxicity data are lacking, these assessments then estimate chronic thresholds indirectly by applying highly conservative safety factors (often poorly-grounded) to acute values, often without mechanistic justification.[10,11] Such approaches cannot account for temporal fluctuations in contaminant bioavailability driven by changing environmental conditions.[12–16]

Process-based toxicokinetic-toxicodynamic (TKTD) models address these limitations by linking external contaminant concentrations to internal body burdens, and resulting adverse effects over time.[17] They integrate concentration, exposure duration, and biological response into a unified framework,[18] allowing chronic thresholds to be derived directly from time-resolved data. While widely applied in water-only systems,[19–21] TKTD modeling in sediments is limited,[17] largely because benthic exposures are complex. For benthic invertebrates, uptake can occur from overlying water, porewater, and ingested particles, thus bioavailability is strongly influenced by contaminant partitioning and speciation.[22] These factors make it difficult to obtain the high-quality, process-resolved dataset required for model parameterization and bioavailability prediction.

Recent studies suggested that isotope tracing is highly effective in laboratory water exposure experiments for generating kinetic data that are categorially needed for modeling.[23,24] However, directly amending kilograms of sediments with stable or radioactive isotopes can be costly and may not reproduce natural binding phases,[25–27] reducing the realism and practicality of sediment exposure experiments.

To overcome these limitations, here we propose a novel isotope-tracing strategy tailored for sediment studies. Rather than spiking isotopes into sediments, organisms are pre-enriched with a stable isotope before exposure to contaminated sediments. By tracking the depuration of the labeled isotope and the simultaneous accumulation of ambient contaminant from sediments, this method provides the process resolution necessary for TKTD parameterization.

To further reduce the model complexity, we characterized the bioavailable contaminant pool in sediments and incorporated it as a proxy source for the metals available to biota. This was achieved by a passive sampling technique —diffusive gradients in thin-films (DGT),[28,29] which quantifies the labile metal species, including both dissolved and dissociable particulate metal forms.[30] While DGT-labile metals have been tested as a proxy for bioavailable metal pool in sediment in fixed-duration assessments,[31–34] their integration into kinetic modeling remains unexplored.

Accordingly, the objectives of this study were to develop the TKTD modeling for sediments by integrating this new isotope-tracing approach with DGT-based bioavailability characterization. Using copper (Cu) as a model metal contaminant of high ecological concern,[35–37] we exposed the estuarine benthic clam *Ruditapes philippinarum,* an ecologically

representative species that integrates particle- and water-mediated exposure pathways in surficial sediments. By establishing mechanistic chronic toxicity thresholds for management purposes, this study offers a process-based framework for sediment risk assessment, adaptable to dynamic estuarine environments and capable of evaluating the fate and risk of contaminants under varying environmental scenarios.

2. Materials and Methods

2.1 Cu-spiked sediment

Plastic containers were cleaned following laboratory protocols to minimize metal contamination (Note S1, Supporting Information, SI). Coastal water, benthic clams (*Ruditapes philippinarum*), and clean sediments were collected and processed as detailed in SI Note S1.

To examine the effects of Cu speciation and concentration on bioaccumulation and toxicity, sediments were spiked with three Cu forms representing typical speciation and concentrations in oxic/sub-oxic sediments: (1) basic Cu carbonate ($Cu_2(OH)_2CO_3$; Ref-0: 0, Low: 300, High: 1300 mg kg^{-1}, dry mass basis), (2) copper chloride ($CuCl_2$; Low: 300, Medium: 600, High: 900 mg kg^{-1}), and (3) Cu adsorbed onto Fe oxyhydroxide (Cu-HFO; Low: 300, Medium: 600, High: 1200 mg kg^{-1}). $Cu_2(OH)_2CO_3$, a common Cu precipitate in natural sediments,[38] represents Cu carbonate and hydroxide species. $CuCl_2$, used in laboratory spiking studies, represents soluble Cu^{2+} species and short-term sediment-bound Cu.[25] Cu-HFO, the adsorbed Cu phase, was prepared at half-, full-, and 2-fold oversaturation relative to Fe oxyhydroxide based on a Cu: Fe saturation curve (SI Figure S1, Note S2). All sediments

were spiked, homogenized, and equilibrated for short term (3 days) to preserve the initial speciation, then equilibrated under seawater for 24-h before the clam exposure experiments (SI Notes S1).

2.2 TKTD measurements using stable-isotope tracing for sediment contamination

We first developed a novel stable-isotope tracing technique to generate a TKTD dataset in sediments, which involves two main stages (Figure 1a): (1) isotope pre-labeling of clams and (2) exposure to Cu contaminated sediments.

2.2.1 Isotope-labeling stage

Isotope-labeling was achieved by exposing the clams to ^{65}Cu-enriched seawater (purity 99.7%, purchased from Isoflex USA) to elevate the tissue ^{65}Cu levels. In a flow-through system, 240 clams were held in a 20-L chamber with 10 μg L^{-1} ^{65}Cu for 7 days (Figure 1a), with water renewed twice daily. Daily water samples were acidified with "1+1" HNO_3 to pH < 2 for ^{65}Cu analysis. During labeling, clams were transferred daily to a separate container for 1 h feeding, rinsed twice with clean seawater to remove algae, and returned to the system.

To evaluate the effectiveness of ^{65}Cu labeling, 10 clams were sampled on Days 1, 3, and 7. Soft tissues were immersed in 1 mmol L^{-1} EDTA for 1 min to remove loosely-associated metals, rinsed, frozen (–20°C), freeze-dried, digested, and analyzed for Cu isotopes. Ten non-labeled clams were also processed and analyzed for background Cu composition.

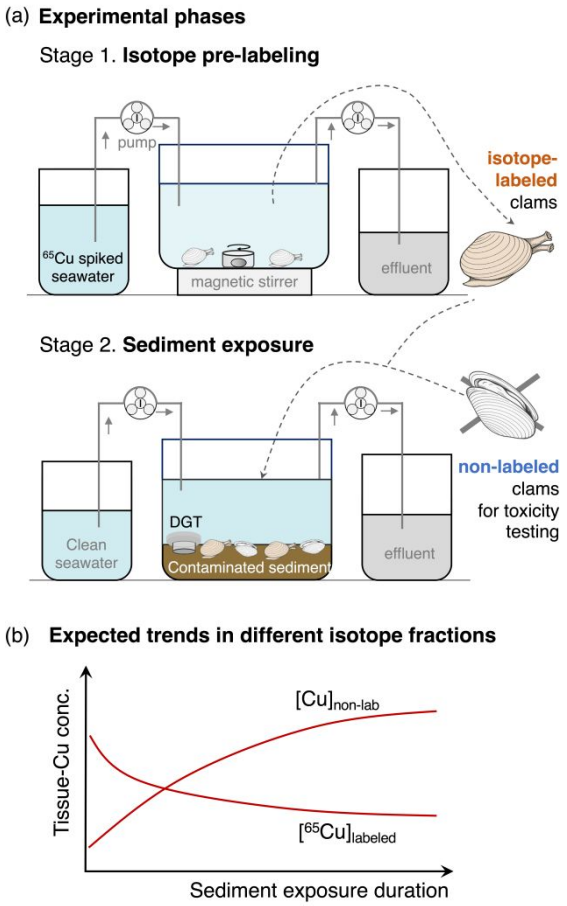

Figure 1. Schematic illustration of experimental procedures and isotope tracing principle. (a) Overview of the stable isotope tracing approach, consisting of the isotope pre-labeling stage and the contaminated sediment exposure stage. (b) Expected trends in tissue concentrations of labeled ^{65}Cu ($[^{65}Cu]_{labeled}$) and ambient non-labeled Cu ($[Cu]_{non\text{-}lab}$).

2.2.2 Sediment exposure stage

After labeling, clams were rinsed and transferred to Cu-spiked sediment chambers for sediment exposure (Figure 1a). Sediment exposure was conducted in 27 plastic chambers (30 × 20 × 17 cm, 3 replicates × 9 Cu spike treatments). Each chamber was filled with 1-cm sediment layer and 10-cm overlying seawater. The water was connected to a flow-through system with 24-h turnover. Continuous aeration was supplied to ensure water mixing. To further reduce Cu accumulation in the overlying water, a manual water renewal was performed daily during clam and sediment sampling.

At the commencement of sediment exposure (Day 0), thirty clams (20 labeled and 10 non-labeled) were introduced to each chamber. Non-labeled clams were marked for identification. Within 30 minutes, clams burrowed partially or completely into sediment.

Exposure lasted up to 14 days or until complete mortality, which occurred in two $CuCl_2$ treatments and one Cu-HFO treatment. For toxicokinetic (TK) assessment, two isotope-labeled clams per replicate were sampled on Days 0.5, 1, 2, 4, 6, 8, 11, and 14. For toxicodynamic (TD) assessment, non-labeled clam survival was monitored every 12 h, with dead individuals removed.

During clam exposure, piston-type chelex-DGT samplers (DGT® Research Ltd.) were deployed in Cu-spiked sediments on Days 0, 2, 4, 6, 8, and 11, and retrieved on Days 2, 4, 6, 8, 11, and 14, respectively. These samplers were inserted face-down to ~0.5 cm sediment depth to accumulate Cu from porewater and loosely sediment-bound sediment fractions (SI Note S3). After retrieval, samplers were rinsed and stored for further processing. In the reference sediment, DGTs remained deployed for the full 14-d duration.

Alongside DGT retrieval, sediment samples (~ 5 g) were collected from multiple chamber locations, homogenized, and centrifuged (3000 × g, 5 min). The resulting supernatant porewater was filtered (0.45 μm), acidified (pH < 2), and stored for Cu analysis. Remaining sediment in the centrifuge tube was preserved for extraction-based speciation analysis (Section 2.3 and SI Note S4).

Overlying water was sampled daily before and after water renewal. From each treatment, 3 mL per replicate was filtered, combined, acidified, and stored for analysis.

2.3 Sampling and analysis

Bulk clean sediment was characterized for particle size and total recoverable metal (TRM) concentrations. Sediments from exposure chambers were analyzed for Cu speciation: TRM, dilute-acid extractable metals (AEM), acid volatile sulfide (AVS), and a modified BCR sequential extraction (exchangeable, reducible, oxidizable, and residual fractions).[39–41] TRM, AVS, and full BCR were measured at the start and end of exposure; AEM and the first-step BCR extraction for exchangeable fraction were determined at multiple time points. More details on sediment analysis are detailed in SI Note S4.

DGT samplers were disassembled, and binding gels digested in 1 mL 1-M HNO_3 for at least 24 h. The eluates were diluted with 2% HNO_3 for Cu analysis and DGT-labile Cu concentration was computed based on equations recommended by the manufacture (SI Note S3).

Sampled clams were processed to clear gut contents, involving a 2-h depuration in clean seawater after vigorous shaken (~120 strokes min^{-1} for 1 minute) in a closed container (effectiveness was confirmed by tissue digest clarity). Clams were then dissected, and soft tissues were freeze-dried, cold-digested overnight in 1.5 mL 65% HNO_3 (ANPEL Laboratory Technologies, Shanghai), and then hot-digested at 80°C for 8 h. Solutions were diluted with deionized water for Cu isotope analysis. Standard reference material (SRM 2976, mussel tissue) was processed identically to verify recovery.

Cu isotopes (^{63}Cu and ^{65}Cu) in sediment digest, water samples, tissue digests, and DGT eluents were quantified by inductively coupled plasma mass spectrometry (ICP−MS,

NexION 2000, PerkinElmer). Comprehensive quality assurance and quality control procedures are described in SI Note S4.

2.4 Data analysis for isotope tracing

Cu in isotope-labeled clams was divided into two fractions (SI Figure S2): the newly accumulated ^{65}Cu ($[^{65}Cu]_{labeled}$), and the non-labeled Cu fraction ($[Cu]_{non\text{-}lab}$) that includes both background Cu and Cu accumulated from sediments with natural isotopic composition.

These fractions were quantified based on isotope-specific analysis (SI Figure S2 illustrates the principle). The non-labeled Cu concentration was calculated from the ICP-MS reported Cu concentration using ^{63}Cu as the quantifying isotope:

$$[Cu]_{non\text{-}lab} = [^{63}Cu]_{ICP\text{-}MS} \quad (1)$$

where $[^{63}Cu]_{ICP\text{-}MS}$ (μg g^{-1} dry weight) is the tissue concentration from ICP-MS reported value, adjusted for digestion volume and dilution.

In contrast, the newly accumulated ^{65}Cu was calculated as the difference between Cu concentrations reported using ^{65}Cu and ^{63}Cu as quantifying isotopes, multiplied by 30.8% (the natural abundance of ^{65}Cu):

$$[^{65}Cu]_{labeled} = \left([^{65}Cu]_{ICP\text{-}MS} - [^{63}Cu]_{ICP\text{-}MS}\right) \times 30.8\% \quad (2)$$

where $[^{65}Cu]_{ICP\text{-}MS}$ (μg g^{-1} dry weight) is also converted to tissue concentration based on digestion and dilution steps. For further methodological details, see our previous publications.[16,42]

2.5 TKTD modeling

The toxicokinetic-toxicodynamic (TKTD) model was used to simulate Cu bioaccumulation and toxicity effects on clam survival.[18,43] The model consists of a TK module for Cu uptake and elimination, and a TD module linking internal Cu concentrations to mortality.

During sediment exposure, $[^{65}Cu]_{labeled}$ was expected to decline due to elimination, while $[Cu]_{non\text{-}lab}$ was expected to increase due to accumulation from sediment (Figure 1b). These processes were modeled using a one-compartment TK model:[44,45]

$$\frac{dC_{int}(t)}{dt} = J_{in}(t) - k_e \cdot C_{int}(t) \quad (3)$$

where $C_{int}(t)$ (μg g^{-1} dry weight) is the internal Cu concentration at time t (d), $J_{in}(t)$ (μg g^{-1} d^{-1}) is the Cu uptake rate, and k_e (d^{-1}) is the elimination rate constant. Growth dilution effect was negligible compared to Cu efflux (SI Figure S3), and was not considered in the model.

Cu uptake was modeled using DGT-labile Cu (C_{DGT}, μg L^{-1}) as a proxy for Cu available to clams:

$$J_{in}(t) = k_{DGT} \times C_{DGT}(t) \quad (4)$$

where k_{DGT} (L g^{-1} d^{-1}) is the uptake rate constant of DGT-labile Cu. TK modeling was later improved with a unified uptake rate formula for better prediction across different Cu speciation and concentrations, as discussed in Section 3.4.2.

Cu-induced mortality in non-labeled clams was simulated with a threshold-based TD model:[19,44]

$$\frac{dH(t)}{dt} = \begin{cases} k_m \times (C_{int}(t) - C_{IT}) + h_0, & \text{if } C_{int}(t) > C_{IT} \\ h_0, & \text{otherwise} \end{cases} \quad (5)$$

$$S(t) = e^{-H(t)} \quad (6)$$

where $H(t)$ (dimensionless) is the cumulative hazard, $S(t)$ is the survival rate, C_{IT} (μg g^{-1}) is the internal threshold concentration, k_m is the mortality rate constant (g μg^{-1} d^{-1}), and h_0 (d^{-1}) is the background hazard rate (set to 0 due to no mortality in the reference treatment).

2.6 Model parameter estimation

TK parameters (k_e and k_{DGT}) were estimated by fitting model simulations to measured tissue Cu concentrations (as illustrated in Figure 1b). Specifically, k_e was fitted to $[^{65}Cu]_{labeled}$. With k_e fixed, k_{DGT} was then fitted to $[Cu]_{non\text{-}lab}$. TD parameters C_{IT} and k_m were estimated by fitting the whole TKTD model to clam survival in the $CuCl_2$ and Cu-HFO treatments where significant toxicity was observed.

Parameter estimation was conducted using OpenModel 2.4.2 (University of Nottingham). Initial parameter values were obtained using least-squares fitting (the Marquardt algorithm), and then all parameter values were optimized using Markov Chain Monte Carlo (MCMC) method via the Metropolis-Hastings algorithm.

3. Results and Discussion

3.1 Sediment characteristics and Cu speciation in spiked sediments

The clean sediments (used for Cu spike and in the reference treatment) were fine-grained (96% < 170 μm; SI Table S1), with metal concentrations well below sediment quality criteria (SI Table S2). No acid volatile sulfide was detected in the original or Cu-spiked sediment, indicating sub-oxic/oxic conditions. Following spiking, total recoverable Cu (TR-Cu) ranged from 300 to 1300 mg kg^{-1} across the treatments, with minimal Cu loss during the

experiment (SI Figure S4). BCR sequential extraction revealed that spiked Cu was mainly in the exchangeable and reducible fractions, accounting for 84% to 98% of TR-Cu (SI Figure S5). These distributions remained stable over time, as did the dilute-acid extractable Cu (AE-Cu) and BCR-exchangeable Cu (SI Figure S4). The shallow sediment layer and clam bioturbation minimized anoxic zones, preventing sulfide formation.

3.2 Cu concentrations in porewater and overlying water

Porewater Cu concentrations, measured by instantaneous grab sampling (PW-Cu) and passive samplers (DGT-labile Cu) varied across treatments, spanning four orders of magnitude (SI Figure S6). $Cu_2(OH)_2CO_3$ treatments exhibited a modest increase of porewater Cu over time, indicating slow dissolution of $Cu_2(OH)_2CO_3$. $CuCl_2$ treatments exhibited higher and more variable porewater Cu levels. Cu-HFO treatments showed intermediate porewater Cu concentrations that declined during initial sediment ageing and stabilized within 4 days. Cu concentrations in the overlying water (OW-Cu) were influenced by Cu efflux from sediments, water exchange, and manual water renewal (SI Figure S6 and S7).

The wide gradient of Cu concentrations in porewater across treatments reflects differences in Cu speciation. More discussion on Cu mobility in the sediment water system is provided in the SI Note S5. Briefly, PW-Cu and DGT-labile Cu were generally similar in spiked sediments, suggesting efficient replenishment of porewater Cu from the solid phase—unlike in the reference sediment.[30] This implies that Cu dissociation in spiked sediments is an important source of bioavailable metal for benthic organisms, either through direct sediment ingestion or by sustaining porewater Cu at the organism-porewater interface.

3.3 Threshold-like relationships between Cu bioaccumulation and aqueous Cu metrics

Threshold relationships between 4-d tissue Cu and aqueous Cu metrics (OW-Cu, PW-Cu, and DGT-labile Cu) were evident (Figure 2a). Tissue Cu remained low until OW-Cu exceeded 5 μg L^{-1}, or until PW-Cu/DGT-labile Cu surpassed 10 μg L^{-1}. Above these thresholds, tissue Cu increased sharply (Figure 2a). Similar threshold responses have been reported in other benthic invertebrates, particularly for DGT-labile metal fluxes (equivalent to concentrations through mathematical conversion). For instance, Zinc (Zn) accumulation in the clam *Tellina deltoidalis* increased markedly when DGT-Zn flux exceeded ~160 μg h^{-1} m^{-2},[32] with similar thresholds (OW-Zn = 32 μg L^{-1}, DGT-Zn flux = 220 μg h^{-1} m^{-2}) observed for *Hyridella australis*.[46] In the midge *Chironomus tentans*, Cu bioaccumulation increased sharply when DGT-Cu flux exceeded ~20 μg h^{-1} m^{-2}.[47]

In contrast, no consistent trends were observed with solid-phase Cu metrics—including TR-Cu, AE-Cu, or BCR-exchangeable Cu (SI Figure S8a)—indicating that they were less representative of bioavailable Cu.

Consistent with traditional ECx assessments, concentration-effect relationships were analyzed for the 4-d and 6-d toxicity endpoints, and all three aqueous Cu metrics showed clear dose-response relationships with survival (Figure 2b), while sediment-phase Cu concentrations were poorly correlated (SI Figure S8b). A two-parameter log-logistic model (SI Note S6) described these relationships, with high goodness-of-fit (Nash-Sutcliffe efficiency, NSE > 0.83) for all aqueous Cu metrics. The median lethal concentrations (LC_{50}) declined with exposure duration, consistent with time-dependent toxicity. Specifically, LC_{50}

values at day 6 (LC_{50}-6d) were 23 μg L^{-1} (OW-Cu), 194 μg L^{-1} (PW-Cu), and 155 μg L^{-1} (DGT-labile Cu) were lower than the corresponding values at day 4 (LC_{50}-4d), which were 102, 1800, and 1160 μg L^{-1}, respectively.

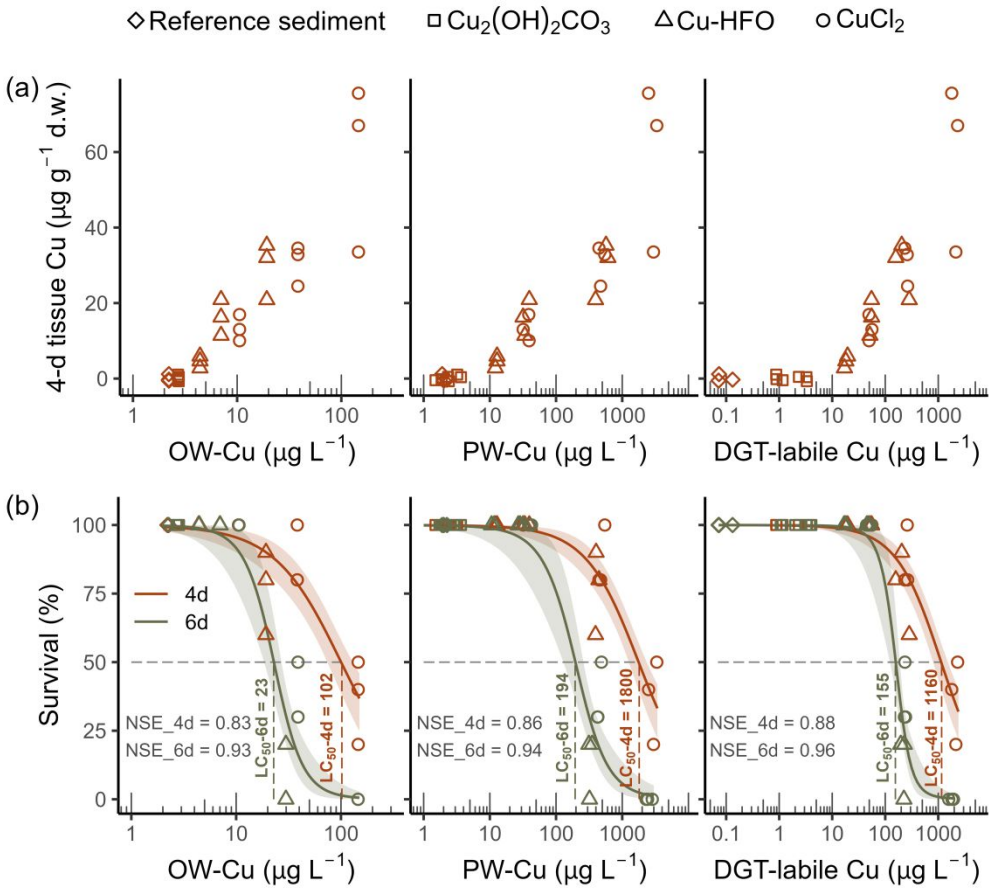

Figure 2. Exposure-duration specific static assessment of Cu bioaccumulation and toxicity using aqueous metrics: overlying water Cu (OW-Cu), porewater Cu (PW-Cu), and DGT-labile Cu. (a) Tissue Cu concentrations on Day 4 showing a threshold-like pattern in relation to aqueous Cu concentrations. Points represent mean tissue Cu concentrations from replicate chambers; point shape distinguishes treatments. (b) Clam survival on Days 4 and 6 as a function to aqueous Cu concentrations. Points represent survival in replicate chambers; solid curves represent log-logistic regression, with shaded areas indicating 95% confidence intervals. Vertical dashed lines indicated LC_{50} values. NSE (Nash–Sutcliffe efficiency) is a goodness-of-fit metric comparing model predictions to observations（$-\infty$ to 1.00, with 1.00 indicating a perfect fit).

3.4 Toxicokinetic-toxicodynamic (TKTD) modeling

3.4.1 Cu elimination

After 7 days of aqueous labeling, clams accumulated ~3.6 µg g^{-1} of ^{65}Cu in tissue ($[^{65}Cu]_{labeled}$) (SI Figure S9). During subsequent sediment exposures, $[^{65}Cu]_{labeled}$ declined exponentially as expected, with the elimination rate slowing over time (Figure 3). After 14-days, final $[^{65}Cu]_{labeled}$ ranged from 0.5 to 1.3 µg g^{-1}, and slightly higher values (1.6–1.9 µg g^{-1}) were observed in treatments terminated early due to toxicity ($CuCl_2$-Medium, $CuCl_2$-High, Cu-HFO-High).

A one-compartment TK model, assuming first-order kinetics, provided a good fit to the measured $[^{65}Cu]_{labeled}$ in clams (Figure 3), with the measured and predicted results aligning with the 1:1 line and within a two-fold deviation (SI Figure S10). The estimated efflux rate constant of $k_e = 0.152 \pm 0.007$ d^{-1} indicates that ~15% of tissue Cu was eliminated daily. This consistent elimination rate across treatments—regardless of sediment Cu speciation or observed toxicity—suggests that Cu excretion was largely independent of exposure type or organism health.

Efflux rate constants during sediment exposure are rarely reported, yet the k_e value obtained here aligns with literature estimates for benthic clams during water-based exposure: *Ruditapes philippinarum* (0.147 ± 0.026 d^{-1}) [48] and *Ruditapes decussatus* (0.143 d^{-1}).[49] The similarity of these k_e values support the interpretation that Cu elimination is a physiological trait largely unaffected by exposure medium.[50,51] Consequently, in the absence of sediment-based k_e values, estimates from aqueous exposures may serve as reasonable surrogates.

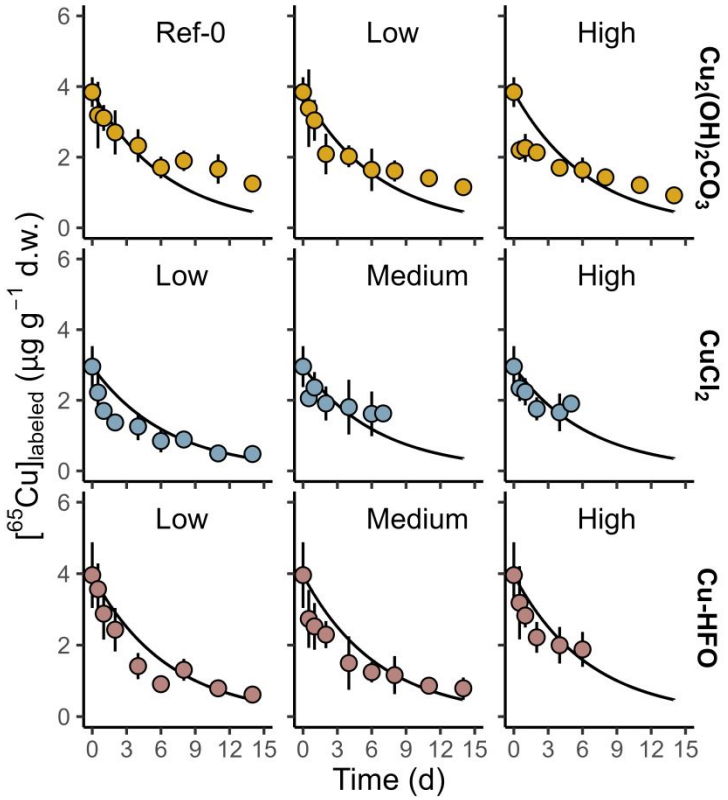

Figure 3. Consistent ^{65}Cu depuration kinetics in sediments across treatments, with a unified elimination rate constant (k_e = 0.152 d^{-1}). Solid points and error bars represent mean remaining pre-labeled ^{65}Cu concentration in clams ($[^{65}Cu]_{labeled}$) and standard deviation of triplicates. Black curves show TK model-predicted ^{65}Cu concentrations with a unified k_e.

3.4.2 Cu bioaccumulation

Non-labeled Cu accumulation ($[Cu]_{non\text{-}lab}$) represents the net result of Cu uptake and elimination, with sediment Cu concentration and speciation being major influencing factors (Figure 4). In unspiked reference sediment (Ref-0), $[Cu]_{non\text{-}lab}$ remained stable at ~3.0 µg g^{-1} over 14 days, indicating no net Cu accumulation. Unlike the elimination of pre-labeled ^{65}Cu, the background Cu pool was not cleared from tissues, suggesting that it represents a metabolically inert fraction. This distinction may be due to different Cu storage speciation in organism tissue: X-ray absorption spectroscopy studies in oysters have found that

background Cu in uncontaminated oysters typically occurs as Cu(I) bound to thio ligands (more tightly bound), while newly accumulated Cu in contaminated oysters appears as Cu(II) coordinated to O/N ligands.[52] These differences in speciation likely explain the low elimination of background Cu.

In $Cu_2(OH)_2CO_3$-spiked sediments, bioaccumulation was limited (Figure 4): $[Cu]_{non\text{-}lab}$ remained stabled in Low treatment and comparable to Ref-0, indicating that influx did not exceed efflux. A slight increase in $[Cu]_{non\text{-}lab}$ occurred in High treatment (from 3 to 6.2 µg g^{-1}). In contrast, $CuCl_2$-spiked sediments induced substantial and dose-dependent Cu accumulation (Figure 4). $[Cu]_{non\text{-}lab}$ increased to 30, 60, and 90 µg g^{-1} within 14, 7, and 6 days for the Low, Medium, and High treatments, respectively. Cu-HFO treatments showed intermediate accumulation levels, varying with Cu loading and HFO sorption saturation (Figure 4). In Low treatment (half-saturated), $[Cu]_{non\text{-}lab}$ increased to 25 µg g^{-1} over 14 days. In Medium (saturated) and High (oversaturated) treatments, $[Cu]_{non\text{-}lab}$ reached 40 and 60 µg g^{-1} over 14 and 6 days, respectively.

Using the pre-determined efflux rate constant (k_e), we first applied a "local fit" approach to model $[Cu]_{non\text{-}lab}$ individually for each treatment, yielding condition-specific uptake rate constants (k_{DGT}), which ranged from 7.2 to 0.01 L g^{-1} d^{-1} (SI Table S3). These constants decreased by three orders of magnitude as C_{DGT} increased by five orders (SI Figure S11). This model described the measured data well within each condition, but its prediction capability was limited due to the need for concentration-specific calibration of k_{DGT} parameters. Furthermore, in low-accumulation treatments (Ref-0 and $Cu_2(OH)_2CO_3$-Low),

limited accumulation of $[Cu]_{non\text{-}lab}$ indicates negligible Cu bioavailability, contradicting with the high k_{DGT} values (SI Figure S11) implying high Cu bioavailability.

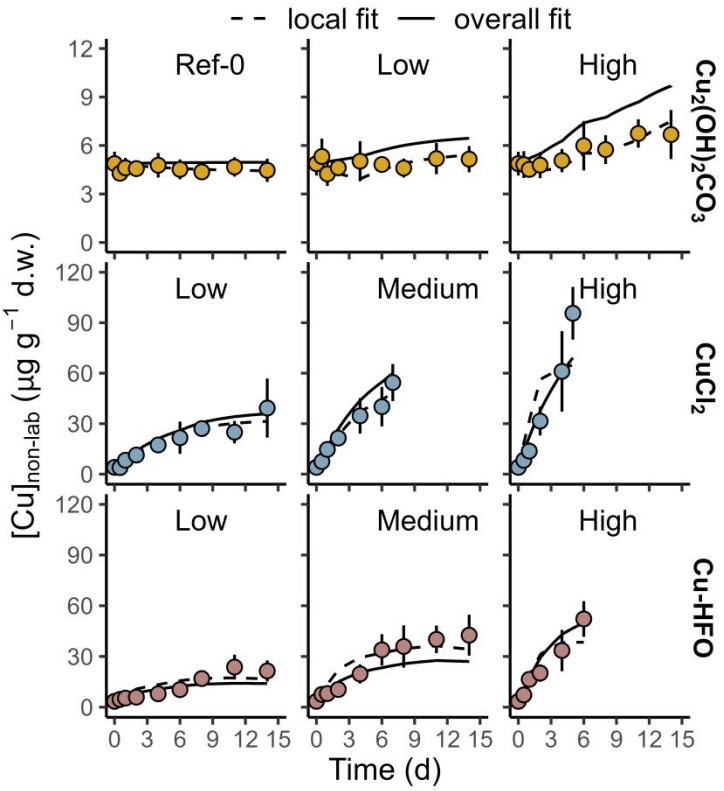

Figure 4. Temporal accumulation of non-labeled Cu in clams, influenced by sediment Cu concentration and speciation. Solid points and error bars represent mean non-labeled Cu concentrations in clams and standard deviation of triplicates. Curves show TK model predictions based on local fits (using condition-specific k_{DGT} values) or an overall fit from a BLM-based TK model.

To address these limitations, we developed a biotic ligand model (BLM)-based TK framework, modeling the Cu uptake rate (J_{in}, µg g^{-1} d^{-1}) as a function of C_{DGT} using a Michaelis-Menten-type relationship (SI Note S7 for model derivation):

$$J_{in}(t) = \frac{J_{max} \cdot K^{CuBL} \cdot C_{DGT}(t)}{1 + K^{CuBL} \cdot C_{DGT}(t)} \quad (7)$$

where J_{max} (µg g^{-1} d^{-1}) is the maximum Cu uptake rate, and K'_{CuBL} (L µg^{-1} or L mol^{-1}) is the conditional Cu-ligand binding constant.

To account for the metabolically inert background Cu (C_{int}^{bkg}) and the exchangeable Cu pool (C_{int}^{exch}), the total tissue (C_{int}^{tot}) was modeled as:

$$\frac{dC_{int}^{exch}}{dt} = J_{in} - k_e \cdot C_{int}^{exch} \quad (8)$$

$$C_{int}^{tot} = C_{int}^{exch} + C_{int}^{bkg} \quad (9)$$

where C_{int}^{bkg} (μg g^{-1}) is set as the mean $[Cu]_{non\text{-}lab}$ at the beginning of the sediment exposure phase.

The unified sediment TK model provided an "overall fit" across all exposure conditions, accurately capturing the relationship between J_{in} and C_{DGT} (NSE = 0.94, SI Figure S12) and reproducing $[Cu]_{non\text{-}label}$ (overall fit, Figure 4). The "overall fit" model demonstrated comparable performance (R^2 = 0.86 vs. 0.89; SI Figure S13), offering broader applicability across sediment conditions.

This model yielded parameter values at J_{max} = 20.2 μg g^{-1} d^{-1} and K'_{CuBL} = 0.0075 L μg^{-1} (equivalent to $10^{5.7}$ L mol^{-1}), which are generally lower than values reported in water-based BLM studies (see SI Note S7 for comparison). This discrepancy may be due to our use of DGT-labile Cu rather than the free Cu^{2+} activity used in water-based studies, which is typically two orders of magnitude lower than measured dissolved Cu concentrations.

3.4.3 Cu toxicity

Clam survival varied with exposure concentrations and Cu speciation (Figure 5). Significant mortality occurred in all $CuCl_2$ treatments and in the Cu-HFO-High treatment, while other treatments showed no observable toxicity (SI Figure S14). In toxic treatments, mortality followed a time-dependent pattern, with survival remaining at 100% initially,

followed by a continuous decline over time. Higher Cu exposures led to earlier onset and faster progression of mortality.

To quantitatively describe the mortality dynamics, we integrated the sediment TK model with a toxicodynamic (TD) model. Model predictions successfully captured the temporal toxicity profiles observed in the $CuCl_2$ and Cu-HFO treatments (NSE = 0.95). The model used a unified set of parameters: an internal threshold concentration (C_{IT} = 30.5 μg g^{-1}) and a mortality rate constant (k_m = 0.0212 g μg^{-1} d^{-1}). When these parameters were applied to the non-toxic treatments, the model correctly predicted the absence of mortality, further validating the TD model (SI Figure S14).

The relatively low C_{IT} value suggests that *R. philippinarum* was sensitive to Cu accumulation, consistent with field reports where maximum tissue concentrations in *R. philippinarum* clams were near or below this threshold, ranging from < 4 to < 38 μg g^{-1}.[53–57] Laboratory bioaccumulation experiments also reported maximum tissue concentrations below this threshold (< 30 μg g^{-1})[58] or slightly above it (< 44 μg g^{-1})[59]. This contrasts with other benthic clam species in similar habitats showing higher Cu tolerance, such as the razor clam *Sinonovacula constricta* (C_{IT} =104–140 μg g^{-1})[60] and the estuarine clam *Potamocorbula laevis* (C_{IT} = 96 and 141 μg g^{-1} in separate studies).[20,61]

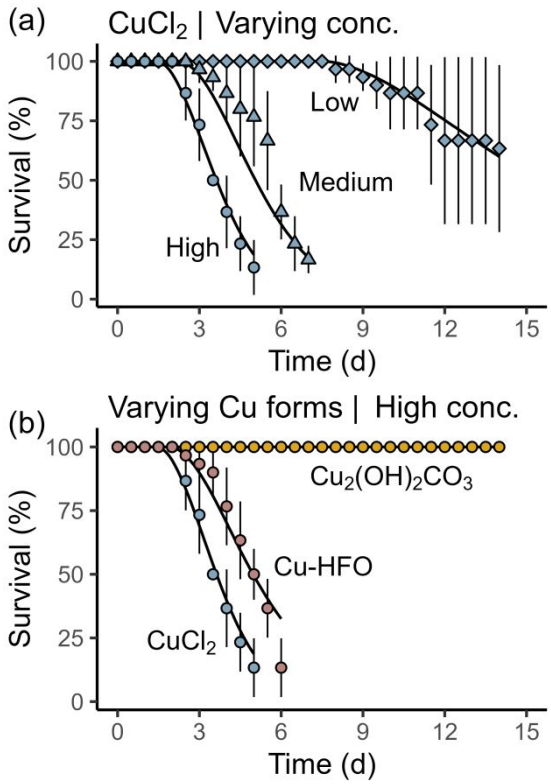

Figure 5. Clam survival varied with sediment Cu concentrations and forms. (a) Effect of Cu exposure concentrations. (b) Effect of Cu forms. Solid points and error bars show mean survival and standard deviation of triplicates. Curves represent model fits.

3.5 Deriving kinetic bioavailability benchmarks with the sediment TKTD model

3.5.1 Estimating DGT-Cu-based LC_{50} in sediments

Using the TKTD model developed in this study (Table 1), we predicted the sediment DGT-labile Cu concentration expected to cause 50% mortality (i.e., DGT-Cu based LC_{50}) across various exposure durations (R code provided in SI Note S8).

Initially, no 50% mortality occurred within the first 3 days due to Cu uptake being constrained by the maximum uptake rate (i.e., saturation effect). As exposure duration increased, the predicted LC_{50} values declined sharply, from 3750 μg L^{-1} at 4 days, to 231 μg L^{-1} at 6 days, and eventually stabilized around 46 μg L^{-1} after 20 days. This steady-state threshold is thus referred to as LC_{50}-chronic value (Figure 6a).

The predicted 6-day LC_{50} (231 μg L^{-1}) matched the empirically derived value 155 ± 30 μg L^{-1} (Figure 2b). However, the predicted 4-day LC_{50} (3750 μg L^{-1}) was higher than the empirical value of 1160 ± 320 μg L^{-1}, likely due to insufficient dose groups, which undermined the precision of the static assessments.

Standard toxicity tests typically use fixed exposure durations (e.g.,10-d) to derive acute endpoints,[39] which differ with duration and hinder cross-study comparisons. Chronic endpoints indirectly extrapolated from these acute values face the same limitation. In contrast, the TKTD model provides a time-independent, mechanistically grounded chronic endpoint—the DGT-Cu-based LC_{50}-chronic = 46 μg L^{-1} for *R. philippinarum*. This metric can be integrated into broader ecological risk assessments, such as constructing species sensitive distribution curves, to estimate hazardous concentrations that protect a defined proportion of species (e.g., HC_5 for 95% species protection).

Table 1. Parameters of sediment TKTD Model

Parameter	Unit	Equations or values
J_{in}	μg g^{-1} d^{-1}	$J_{in} = \frac{J_{max} \cdot K^{CuBL} \cdot C_{DGT}}{1 + K^{CuBL} \cdot C_{DGT}}$
J_{max}	μg g^{-1} d^{-1}	20.2 ± 5.9
K'_{CuBL}	L μg^{-1}	0.0075 ± 0.0013
k_e	d^{-1}	0.152 ± 0.007
C_{IT}	μg g^{-1}	30.5 ± 0.2
k_m	g μg^{-1} d^{-1}	0.0212 ± 0.0005

3.5.2 Estimating DGT-Cu-based NEC in sediments

The DGT-Cu-based no-effect concentration (NEC_{DGT}) represents the highest DGT-labile Cu concentration in sediment that does not cause mortality under prolonged exposure. Within the TKTD framework, NEC_{DGT} is estimated under two assumptions: (1) Cu bioaccumulation reaches steady state ($\frac{dC_{int}(t)}{dt} = 0$), and (2) the internal Cu concentration remains below the toxicity threshold ($C_{int} \leq C_{IT}$). NEC_{DGT} is obtained by solving the equation:

$$C_{IT} = \frac{J_{max} \times K^{CuBL} \times NEC_{DGT}}{(1 + K^{CuBL} \times NEC_{DGT}) \times k_e} \quad (10)$$

Using model parameter values (Table 1), the NEC for DGT-labile Cu was estimated at 40 μg L^{-1} (Figure 6b). Below this threshold, Cu exposure is predicted to not cause any mortality in *R. philippinarum*.

This NEC pertains specifically to survival and may not protect against sublethal effects like impaired growth or reproduction, which often occur at lower concentrations. Nonetheless, this survival-based NEC, combined with the operational simplicity and time-integrating capability of the DGT technique, serves as a valuable screening tool.

If NEC_{DGT} are established for more sensitive species or conservation priorities (e.g., endangered species), this metric can guide early-stage site assessments, flagging high-risk sediments for further management. Thus, this TKTD-derived NEC bridges mechanistic toxicology with practical sediment quality diagnostics, enabling more biologically relevant environmental assessments.

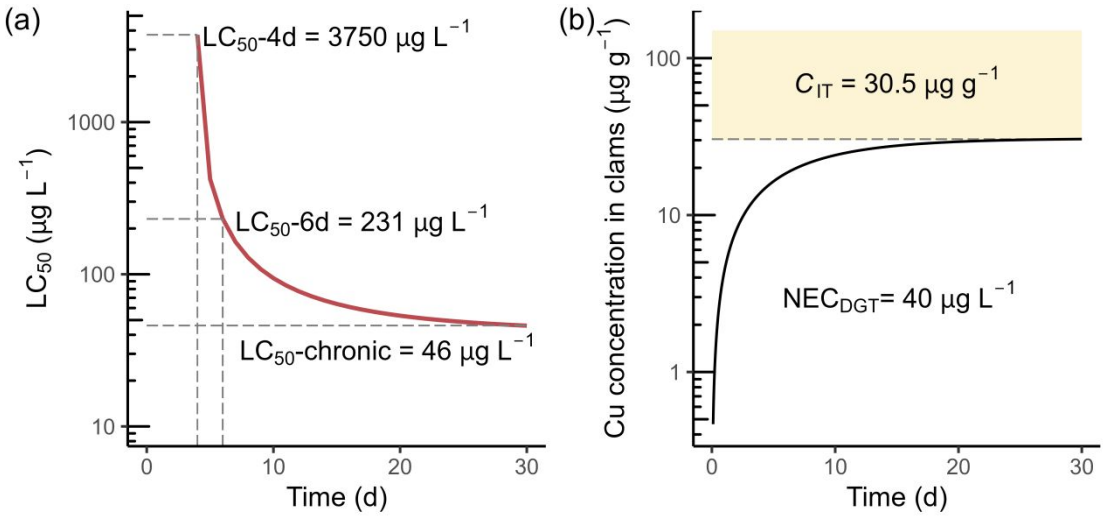

Figure 6. Kinetic bioavailability benchmarks from sediment TKTD models for *R. philippinarum*, including DGT-Cu based chronic median lethal concentration (LC_{50}-chronic) and no-effect concentration (NEC_{DGT}). (a) Time-varying LC_{50} curve; (b) Derivation of NEC_{DGT} (40 µg L^{-1}). Black curve shows Cu accumulation in clams (C_{int}), remaining below the internal threshold level (C_{IT}) during prolonged exposure to DGT-labile Cu concentrations of 40 µg L^{-1}.

3.6 Bioavailability as a kinetic process: implications for sediment quality benchmarking

Environmental risk assessments typically assume equilibrium conditions,[63] yet contaminant exposure in real-world is dynamic. Traditional methods for characterizing sediment contaminant bioavailability, such as porewater analysis or solid-phase extraction, are widely used for their practicality.[9] However, these methods often oversimplify the temporal complexity of exposure.

Static assessments, such as short-term bioassays, are constrained by their fixed-time design and often fail to capture the dynamic nature of contaminant accumulation and toxicity. The threshold values (ECx) derived from these assessments are dependent on the exposure duration and may not remain relevant under prolonged exposure.[64–66] Furthermore,

bioaccumulation tests alone cannot identify the internal contaminant dose that trigger toxicity. In our study, a tissue Cu concentration above ~35 μg g^{-1} was associated with over 50% mortality by day 4 (Figure 2a and 2b). However, this threshold could vary across different exposure scenarios due to changes in subcellular partitioning patterns, which influence the proportion of metabolically available versus detoxified Cu.[67] Without concurrent toxicity testing, this critical thresholds remain unclear. This disconnect may explain why tissue residue data are underused in sediment risk assessments.[39,50]

To address these gaps, we developed a sediment TKTD model that mechanistically reframe bioavailability as a dynamic, kinetic property. Using DGT-labile Cu to represent the bioavailable Cu pool, along with a stable-isotope tracing technique, we derived kinetics-based chronic bioavailability benchmarks, such as DGT-labile Cu-based LC_{50}-chronic and NEC_{DGT}. These new benchmarks are grounded in mechanistic processes and account for prolonged exposure effects, providing more informative metrics than those indirectly estimated in conventional studies. Notably, the DGT technique integrates time-dependent measurements of labile metals, combing kinetic relevance with operational simplicity. This ensures that the derived LC_{50} and NEC values are both scientifically robust and compatible with existing monitoring protocols,[33] making them suitable for inclusion in regulatory sediment quality assessments.

Although our model implicitly assumes constant exposure, it is not a necessity, and the model can be adaptable to more variable conditions, such as variations in salinity,[45] temperature,[68] or hydrodynamics[69], all of which influence metal chemistry and organism

physiology. By establishing relationships between these variables with TKTD parameters, the model can offer more accurate insights into bioavailability dynamics, supporting the development of context-sensitive, bioavailability-based sediment quality benchmarks that reflect both exposure duration and environmental variability.[17]

This study introduces a mechanistic framework for assessing the risks posed by metal-contaminated sediments. The stable-isotope tracing technique generates high-quality data for resolving bioaccumulation kinetics in sediment environments, while DGT measurements simplify exposure scenarios, enabling direct modeling without the complexity of multiple exposure routes. The model's time-integrated, process-based benchmarks enhance the kinetic understanding of bioavailability, offering a scientifically grounded concept of bioavailability highly relevant for environmental management in dynamic estuarine ecosystems.

Notes

The authors declare that they have no known competing financial interests or personal relationships that could have appeared to influence the work reported in this paper.

ACKNOWLEDGEMENTS

We thank Dr. Fang Wu for her assistance with the ICP-MS analysis, Hongkai Wang and Yiran Shi for their help with the laboratory experiment. This study was supported by the National Natural Science Foundation of China (Grant No.42477281, 42377267).

Reference

(1) Burton, G. A. Metal bioavailability and toxicity in sediments. *Crit. Rev. Environ. Sci. Technol.* **2010**, *40* (9–10), 852–907.

(2) Jin, Z.; Ding, S.; Sun, Q.; Gao, S.; Fu, Z.; Gong, M.; Lin, J.; Wang, D.; Wang, Y. High resolution spatiotemporal sampling as a tool for comprehensive assessment of zinc mobility and pollution in sediments of a eutrophic lake. *J. Hazard. Mater.* **2019**, *364*, 182–191.

(3) Chapman, P. M.; Wang, F.; Janssen, C.; Persoone, G.; Allen, H. E. Ecotoxicology of metals in aquatic sediments: Binding and release, bioavailability, risk assessment, and remediation. *Can. J. Fish. Aquat. Sci.* **1998**, *55*, 2221–2243.

(4) Griscom, S. B.; Fisher, N. S. Bioavailability of sediment-bound metals to marine bivalve molluscs: An overview. *Estuaries* **2004**, *27* (5), 826–838.

(5) Long, E. R. Spatial extent of sediment toxicity in U.S. estuaries and marine bays. *Environ. Monit. Assess.* **2000**, *64*, 391–407.

(6) Oliver, L.; Sinnathamby, S.; Purucker, S.; Raimondo, S. A probabilistic approach to chronic effects assessments for listed species in a vernal pool case study. *Integr. Environ. Assess. Manag.* **2024**, *20* (5), 1654–1666.

(7) Di Toro, D. M.; Mahony, J. D.; Hansen, D. J.; Scott, K. J.; Carlson, A. R.; Ankley, G. T. Acid volatile sulfide predicts the acute toxicity of cadmium and nickel in sediments. *Environ. Sci. Technol.* **1992**, *26* (1), 96–101.

(8) USEPA. *Procedures for the Derivation of EquilibriumPartitioning Sediment Benchmarks (ESBs) for the Protection of BenthicOrganisms: Metal Mixtures (Cadmium, Copper, Lead, Nickel, Silver and Zinc)*; US EnvironmentalProtection Agency, Office of Research and Development: Washington, DC, USA, **2005**.

(9) Burgess, R. M.; Berry, W. J.; Mount, D. R.; Di Toro, D. M. Mechanistic sediment quality guidelines based on contaminant bioavailability: Equilibrium partitioning sediment benchmarks. *Environ. Toxicol. Chem.* **2013**, *32* (1), 102–114.

(10) Forbes, V. E.; Calow, P. Extrapolation in ecological risk assessment: Balancing pragmatism and precaution in chemical controls legislation. *BioScience* **2002**, *52* (3), 249–257.

(11) Malkiewicz, K.; Hansson, S. O.; Rudén, C. Assessment factors for extrapolation from short-time to chronic exposure—are the reach guidelines adequate? *Toxicol. Lett.* **2009**, *190*, 16–22.

(12) Peiffer, S.; Kappler, A.; Haderlein, S. B.; Schmidt, C.; Byrne, J. M.; Kleindienst, S.; Vogt, C.; Richnow, H. H.; Obst, M.; Angenent, L. T.; Bryce, C.; McCammon, C.; Planer-Friedrich, B. A biogeochemical-hydrological framework for the role of redox-active compounds in aquatic systems. *Nat. Geosci.* **2021**, *14* (5), 264–272.

(13) Xie, M.; Wang, N.; Gaillard, J.-F.; Packman, A. I. Hydrodynamic forcing mobilizes Cu in low-permeability estuarine sediments. *Environ. Sci. Technol.* **2016**, *50* (9), 4615–4623.

(14) Xie, M.; Wang, N.; Gaillard, J.-F.; Packman, A. I. Interplay between flow and bioturbation enhances metal efflux from low-permeability sediments. *J. Hazard. Mater.* **2018**, *341*, 304–312.

(15) Fetters, K. J.; Costello, D. M.; Hammerschmidt, C. R.; Burton Jr., G. A. Toxicological effects of short-term resuspension of metal-contaminated freshwater and marine sediments. *Environ. Toxicol. Chem.* **2016**, *35* (3), 676–686.
(16) Tan, Q.-G.; Lu, S.; Chen, R.; Peng, J. Making acute tests more ecologically relevant: Cadmium bioaccumulation and toxicity in an estuarine clam under various salinities modeled in a toxicokinetic-toxicodynamic framework. *Environ. Sci. Technol.* **2019**, *53*, 2873–2880.
(17) Burgess, R. M.; Kane Driscoll, S.; Bejarano, A. C.; Davis, C. W.; Hermens, J. L. M.; Redman, A. D.; Jonker, M. T. O. A review of mechanistic models for predicting adverse effects in sediment toxicity testing. *Environ. Toxicol. Chem.* **2023**, *43* (8), 1778–1794.
(18) Jager, T.; Albert, C.; Preuss, T. G.; Ashauer, R. General unified threshold model of survival—a toxicokinetic-toxicodynamic framework for ecotoxicology. *Environ. Sci. Technol.* **2011**, *45* (7), 2529–2540.
(19) Tan, Q.-G.; Wang, W.-X. Two-compartment toxicokinetic-toxicodynamic model to predict metal toxicity in *Daphnia magna*. *Environ. Sci. Technol.* **2012**, *46* (17), 9709–9715.
(20) Cao, X.; Yu, Z.-X.; Xie, M.; Pan, K.; Tan, Q.-G. Higher risks of copper toxicity in turbid waters: Quantifying the bioavailability of particle-bound metals to set site-specific water quality criteria. *Environ. Sci. Technol.* **2023**, *57* (2), 1060–1070.
(21) Li, H.; Zhang, Q.; Su, H.; You, J.; Wang, W.-X. High tolerance and delayed responses of *Daphnia magna* to neonicotinoid insecticide imidacloprid: Toxicokinetic and toxicodynamic modeling. *Environ. Sci. Technol.* **2021**, *55* (1), 458–467.
(22) Lee, B.-G.; Griscom, S. B.; Lee, J.-S.; Choi, H. J.; Koh, C.-H.; Luoma, S. N.; Fisher, N. S. Influences of dietary uptake and reactive sulfides on metal bioavailability from aquatic sediments. *Science* **2000**, *287* (5451), 282–284.
(23) Croteau, M.-N.; Luoma, S. N. Delineating copper accumulation pathways for the freshwater bivalve *Corbicula* using stable copper isotopes. *Environ. Toxicol. Chem.* **2005**, *24* (11), 2871–2878.
(24) Wang, W.-X.; Fisher, N. S. Assimilation efficiencies of chemical contaminants in aquatic invertebrates: A synthesis. *Environ. Toxicol. Chem.* **1999**, *18* (9), 2034–2045.
(25) Simpson, S. L.; Angel, B. M.; Jolley, D. F. Metal equilibration in laboratory-contaminated (spiked) sediments used for the development of whole-sediment toxicity tests. *Chemosphere* **2004**, *54* (5), 597–609.
(26) Costello, D. M.; Hammerschmidt, C. R.; Burton, G. A. Copper sediment toxicity and partitioning during oxidation in a flow-through flume. *Environ. Sci. Technol.* **2015**, *49* (11), 6926–6933.
(27) Costello, D. M.; Harrison, A. M.; Hammerschmidt, C. R.; Mendonca, R. M.; Burton, G. A. Hitting reset on sediment toxicity: Sediment homogenization alters the toxicity of metal-amended sediments. *Environ. Toxicol. Chem.* **2019**, *38* (9), 1995–2007.
(28) Zhang, H.; Davison, W. Direct in situ measurements of labile inorganic and organically bound metal species in synthetic solutions and natural waters using diffusive gradients in thin films. *Anal. Chem.* **2000**, *72* (18), 4447–4457.
(29) Davison, W.; Zhang, H. In situ speciation measurements of trace components in natural waters using thin-film gels. *Nature* **1994**, *367* (6463), 546–548.

(30) Harper, M. P.; Davison, W.; Zhang, H.; Tych, W. Kinetics of metal exchange between solids and solutions in sediments and soils interpreted from DGT measured fluxes. *Geochim. Cosmochim. Acta* **1998**, *62* (16), 2757–2770.

(31) Amato, E. D.; Simpson, S. L.; Jarolimek, C. V.; Jolley, D. F. Diffusive gradients in thin films technique provide robust prediction of metal bioavailability and toxicity in estuarine sediments. *Environ. Sci. Technol.* **2014**, *48*, 4485–4494.

(32) Amato, E. D.; Simpson, S. L.; Belzunce-Segarra, M. J.; Jarolimek, C. V.; Jolley, D. F. Metal fluxes from porewaters and labile sediment phases for predicting metal exposure and bioaccumulation in benthic invertebrates. *Environ. Sci. Technol.* **2015**, *49* (24), 14204–14212.

(33) E. D. Amato; T. Bolam; M. J. Belzunce-Segarra. *Guidelines for the Use of Diffusive Gradients inThin Films for Measuring Metal Fluxes in Sediment*. In InternationalCouncil for the Exploration of the Sea: Copenhagen, Denmark, **2019**; Vol.62.

(34) Xie, M.; Simpson, S. L.; Huang, J.; Teasdale, P. R.; Wang, W.-X. In situ DGT sensing of bioavailable metal fluxes to improve toxicity predictions for sediments. *Environ. Sci. Technol.* **2021**, *55* (11), 7355–7364.

(35) Lu, Y.; Wang, P.; Wang, C.; Zhang, M.; Cao, X.; Chen, C.; Wang, C.; Xiu, C.; Du, D.; Cui, H.; Li, X.; Qin, W.; Zhang, Y.; Wang, Y.; Zhang, A.; Yu, M.; Mao, R.; Song, S.; Johnson, A. C.; Shao, X.; Zhou, X.; Wang, T.; Liang, R.; Su, C.; Zheng, X.; Zhang, S.; Lu, X.; Chen, Y.; Zhang, Y.; Li, Q.; Ono, K.; Stenseth, N. C.; Visbeck, M.; Ittekkot, V. Multiple pollutants stress the coastal ecosystem with climate and anthropogenic drivers. *J. Hazard. Mater.* **2022**, *424*, 127570.

(36) Johnson, A. C.; Jin, X.; Nakada, N.; Sumpter, J. P. Learning from the past and considering the future of chemicals in the environment. *Science* **2020**, *367*, 384–387.

(37) Simpson, S. L.; Yverneau, H.; Cremazy, A.; Jarolimek, C. V.; Price, H. L.; Jolley, D. F. DGT-induced copper flux predicts bioaccumulation and toxicity to bivalves in sediments with varying properties. *Environ. Sci. Technol.* **2012**, *46*, 9038–9046.

(38) Flemming, C. A.; Trevors, J. T. Copper toxicity and chemistry in the environment: A review. *Water. Air. Soil Pollut.* **1989**, *44* (1–2), 143–158.

(39) Simpson, S.; Batley, G. *Sediment Quality Assessment: A Practical Guide*; CSIRO Publishing: Melbourne, Victoria,Australia, **2016**.

(40) Simpson, S. L. A rapid screening method for acid-volatile sulfide in sediments. *Environ. Toxicol. Chem.* **2001**, *20* (12), 2657–2661.

(41) Rauret, G.; López-Sánchez, J. F.; Sahuquillo, A.; Rubio, R.; Davidson, C.; Ure, A.; Quevauviller, Ph. Improvement of the BCR three step sequential extraction procedure prior to the certification of new sediment and soil reference materials. *J. Environ. Monit.* **1999**, *1*, 57–61.

(42) Wu, Q.; Zheng, T.; Simpson, S. L.; Tan, Q.-G.; Chen, R.; Xie, M. Application of a multi-metal stable-isotope-enriched bioassay to assess changes to metal bioavailability in suspended sediments. *Environ. Sci. Technol.* **2021**, *55*, 13005–13013.

(43) Ashauer, R.; Escher, B. I. Advantages of toxicokinetic and toxicodynamic modelling in

aquatic ecotoxicology and risk assessment. *J. Environ. Monit.* **2010**, *12*, 2056–2061.
(44) Wang, W.-X.; Tan, Q.-G. Applications of dynamic models in predicting the bioaccumulation, transport and toxicity of trace metals in aquatic organisms. *Environ. Pollut.* **2019**, *252*, 1561–1573.
(45) Zhong, G.; Lu, S.; Chen, R.; Chen, N.; Tan, Q.-G. Predicting risks of cadmium toxicity in salinity-fluctuating estuarine waters using the toxicokinetic-toxicodynamic model. *Environ. Sci. Technol.* **2020**, *54* (21), 13899–13907.
(46) Amato, E. D.; Marasinghe Wadige, C. P. M.; Taylor, A. M.; Maher, W. A.; Simpson, S. L.; Jolley, D. F. Field and laboratory evaluation of DGT for predicting metal bioaccumulation and toxicity in the freshwater bivalve *Hyridella australis* exposed to contaminated sediments. *Environ. Pollut.* **2018**, *243*, 862–871.
(47) He, Y.; Guo, C.; Lv, J.; Hou, S.; Zhang, Y.; Zhang, Y.; Xu, J. Predicting trace metal bioavailability to chironomids in sediments by diffusive gradients in thin films. *Sci. Total Environ.* **2018**, *636*, 134–141.
(48) Pan, K.; Wang, W.-X. Biodynamics to explain the difference of copper body concentrations in five marine bivalve species. *Environ. Sci. Technol.* **2009**, *43* (6), 2137–2143.
(49) Serafim, A.; Bebianno, M. J. Metallothionein role in the kinetic model of copper accumulation and elimination in the clam *Ruditapes decussatus*. *Environ. Res.* **2009**, *109* (4), 390–399.
(50) Luoma, S. N.; Rainbow, P. S. *Metal Contamination in Aquatic Environments*; Cambridge University Press: New York, **2008**.
(51) Wang, W.-X.; Fisher, N. S.; Luoma, S. N. Kinetic determinations of trace element bioaccumulation in the mussel *Mytilus edulis*. *Mar. Ecol. Prog. Ser.* **1996**, *140*, 91–113.
(52) Tan, Q.-G.; Wang, Y.; Wang, W.-X. Speciation of Cu and Zn in two colored oyster species determined by X-ray absorption spectroscopy. *Environ. Sci. Technol.* **2015**, *49* (11), 6919–6925.
(53) Liang, L.; He, B.; Jiang, G.; Chen, D.; Yao, Z. Evaluation of mollusks as biomonitors to investigate heavy metal contaminations along the Chinese Bohai Sea. *Sci. Total Environ.* **2004**, *324* (1–3), 105–113.
(54) Li, Y.; Yu, Z.; Song, X.; Mu, Q. Trace metal concentrations in suspended particles, sediments and clams (*Ruditapes philippinarum*) from Jiaozhou Bay of China. *Environ. Monit. Assess.* **2006**, *121*, 491–501.
(55) Yang, F.; Zhao, L.; Yan, X.; Wang, Y. Bioaccumulation of trace elements in *Ruditapes philippinarum* from China: Public health risk assessment implications. *Int. J. Environ. Res. Public. Health* **2013**, *10* (4), 1392–1405.
(56) Qian, J.; Cao, X.; Xiong, H.; Liu, F.; Xie, M.; Chen, R.; Tan, Q.-G. Hidden threat in turbid waters: Quantifying and modeling the bioaccumulation and risks of particulate metals to clams. *Environ. Pollut.* **2025**, *368*, 125746.
(57) Liu, M. X.; Bao, W. Y.; Zhang, S. L. The seasonal variation of some trace metals in the *Ruditapes philippinus* in Jiaozhou Bay. *Oceanol. Limnol. Sin.* **1983**, *14*, 22–29.
(58) Won, E.-J.; Hong, S.; Ra, K.; Kim, K.-T.; Shin, K.-H. Evaluation of the potential impact

of polluted sediments using manila clam *Ruditapes philippinarum*: Bioaccumulation and biomarker responses. *Environ. Sci. Pollut. Res.* **2012**, *19* (7), 2570–2580.
(59) Santana, L. M. B. M.; Blasco, J.; Abessa, D. M. S.; Campana, O. Bioaccumulation kinetics of copper in *Ruditapes philippinarum* exposed to increasing, continuous and pulsed exposure: Implications for growth. *Sci. Total Environ.* **2017**, *595*, 920–927.
(60) Cai, M.; Ma, T.; Que, H.; Shi, B.; Liu, X.; Ke, Y. Investigating the impact of humic acid on copper accumulation in *Sinonovacula constricta* using a toxicokinetic-toxicodynamic model. *Toxics* **2024**, *12*, 74.
(61) Chen, W.-Q.; Wang, W.-X.; Tan, Q.-G. Revealing the complex effects of salinity on copper toxicity in an estuarine clam *Potamocorbula laevis* with a toxicokinetic-toxicodynamic model. *Environ. Pollut.* **2017**, *222*, 323–330.
(62) Rainbow, P. S. Trace metal concentrations in aquatic invertebrates: Why and so what? *Environ. Pollut.* **2002**, *120* (3), 497–507.
(63) Burton, G. A.; Johnston, E. L. Assessing contaminated sediments in the context of multiple stressors. *Environ. Toxicol. Chem.* **2010**, *29* (12), 2625–2643.
(64) Jager, T. Some good reasons to ban E*Cx* and related concepts in ecotoxicology. *Environ. Sci. Technol.* **2011**, *45* (19), 8180–8181.
(65) Burton Jr., G. A.; Nedrich, S. M. Exposures in aquatic ecosystems: the weak link in risk assessments—a critical perspective. *Ecotoxicol. Environ. Contam.* **2018**, *13* (2), 5–9.
(66) Allen Burton, G. Breaking from tradition: Establishing more realistic sediment quality guidelines. *Environ. Sci. Pollut. Res.* **2018**, *25* (4), 3047–3052.
(67) Campana, O.; Taylor, A. M.; Blasco, J.; Maher, W. A.; Simpson, S. L. Importance of subcellular metal partitioning and kinetics to predicting sublethal effects of copper in two deposit-feeding organisms. *Environ. Sci. Technol.* **2015**, *49* (3), 1806–1814.
(68) Ma, X.; Xiao, W.; Zhang, Q.; Yu, Z.; Jia, X.; Chen, R.; Xie, M.; Tan, Q.-G. Fast in, faster out: Rapid thallium elimination drives low bioaccumulation in coastal gastropods. *Environ. Sci. Technol.* **2025**, *59* (30), 15720–15729.
(69) Xu, D.; Xiong, H.; Wu, Q.; Xiao, W.; Simpson, S. L.; Tan, Q.-G.; Chen, R.; Xie, M. Sediment ballet: Unveiling the dynamics of metal bioavailability in sediments following resuspension and reequilibration. *Environ. Sci. Technol.* **2024**, *58* (51), 22755–22765.